Silicon-Based Micro-structured Sensors for Highly Efficient Thermal Neutron Detectors

Zeshaan H. Shamsi, Rodolfo Rodriguez-Davila, Leunam Fernandez-Izquierdo, Jesus A. Caraveo-Frescas, Manuel A. Quevedo-Lopez*

University of Texas at Dallas

Department of Materials Science & Engineering

800 W. Campbell Rd. Richardson, Tx 75080

Microstructured Neutron Detectors (MSNDs), Thermal Neutron Detection Efficiency, Deep Silicon Etch, Microstructures, Sedimentation, Electron-Hole Pairs (EHPs)

ABSTRACT: This paper demonstrates a simple and manufacturable process compatible with Si-based technology to fabricate micro-structured thermal neutron ($E_{neutron}$ = ~25 meV) sensors featuring 40 μm deep vertically etched silicon micro-structured diodes that are subsequently backfilled with boron-10 (^{10}B) for thermal neutron detection. The trenches were backfilled utilizing with ^{10}B using sedimentation and aerosol methods to accelerate the fabrication process and produce high-yielding thermal neutron detectors. The efficiency of the resulting neutron detectors shows a correlation with trench filling density and uniformity when compared to traditionally gravity-assisted ^{10}B sedimentation. The experimental results are compared and verified with Monte-Carlo Nuclear Particle (MCNP) code simulations. This backfilling process not only produces a conversion layer, but also is used for the conformal doping using a high temperature annealing that improves the reverse bias leakage current in the diodes an increasing in detection efficiency. The resulting devices demonstrate thermal neutron detection efficiencies of up to 25% with active device areas of 210 mm^2.

Introduction:

Neutrons originate from a variety of events, including spontaneous fission decay from heavy elements such as Cf-252 (^{252}Cf) and as by products in certain fusion or fission reactions used in energy generation or weapons of mass destruction respectively. Therefore, its detection and real-time monitoring are very important for nuclear material handling, experimental particle physics as well as for national security.[1] Neutrons can be exceedingly practical for clean energy production but can also be catastrophic if not properly monitored.

Historically, solid-state semiconductor neutron detectors have been used as a potential replacement for conventional traditional gas proportional counters.[1] This has recently accelerated due to the concerns related to the availability of the ^3He gas used in gas proportional counter detectors. Besides concerns related to availability of ^3He, traditional gas-proportional counters based on ^3He gas are bulky, susceptible to magnetic fields, expensive and require high voltage power supplies to operate.[2] Additionally, most of these systems have limitations related to continuous data logging. Availability of ^3He is limited with only 1.38 ppm of the earth's atmosphere.[3] These limitations have increased demand for alternative thermal neutron detectors.[1] Solid-state detectors are an attractive alternative as these detectors have the potential for scalability and portability while maintaining a streamlined fabrication process if traditional silicon fabrication process is used. In this case, the detector size and scalability is only limited to Si-manufacturing wafer size, which is currently 300 mm.

Radiation detectors can be categorized into one of two detection mechanisms: Direct and Indirect detection. Direct detection occurs when the material produces detectable signals from the incident radiation. An indirect detection mechanism requires an intermediate detection step most likely in the form of a moderator or conversion material. This can be in the form of a neutron moderator to decrease the energy of incident neutrons, or scintillation which transforms the incident radiation into optical photons that are more susceptible for detection from the target material and signal processing. Most neutron detectors operate in an indirect detection mode due to neutrons' reduced interaction with matter for being chargeless.[4,5] Scintillation-based detectors, when incident neutrons interact with a scintillation material, photons are produced and subsequently detected using regular silicon photomultipliers. Scintillation based detectors, such as Thallium doped Sodium-Iodide, NaI:Tl and Lithium Thallium doped Sodium-Iodide, NaIL, can also be used for spectroscopy with energy resolutions between 6% – 10%.[6,7] However, these scintillators require high voltage operation, are easily affected by ambient conditions such as humidity which require encapsulation hardware, and the cost per cubic volume exponentially increases with area detection producing a financial barrier to entry.[6–8]

Semiconductor solid-state detectors have a smaller footprint compared to gas proportional and scintillation-based detectors while remaining relatively inexpensive for comparable detection efficiencies. This characteristic is due to the fact that semiconductor solid-state detectors rely on conventional solid-state devices such as PN or Schottky junction-based diodes that operate in reverse bias conditions that increase the depletion zone (detection zone) available for electron-hole pair (EHP) generation by ionizing radiation.[9] Solid-state detectors typically operate on the indirect mode and a neutron conversion material must be used.[4,5] In semiconductor solid-state detectors operating in the indirect mode, probability of interaction of the conversion material with an incident neutron is defined as its neutron capture cross section and is measured in Barnes (1 b = 100 fm^2).

Typically, ^{6}LiF or ^{10}B are chosen for the thermal neutron converting layers given its large thermal neutron cross-section.[10–14] The ^{6}Li-neutron reaction produces a 2.05 MeV alpha particle, which is easier to detect over background radiation; however, ^{6}Li possesses a smaller cross-section (940 b) compared to 3840 b for ^{10}B. On the other hand, the reaction between ^{10}B and a thermal neutron produces a 840 keV ^{7}Li ion and a 1.4 MeV alpha particle. Other material isotopes may possess higher thermal neutron cross sections such has ^{157}Gd, but the product particles have energies rarely exceeding 250 keV, making them difficult to detect over a background noise signal.[11,15] The transmutation reactions for ^{6}LiF, ^{10}B and ^{157}Gd are shown in Equation 1. In all cases, the resulting energetic particles will generate charges as they pass through the diode. The charge produced in the diodes is then collected by a reversed biased diode. ^{10}B's higher natural thermal neutron capture cross section, sufficiently detectable secondary alpha particle generation, and ease of use in application are key factors in choosing the isotope for the neutron conversion material in this paper.

$$a)\ {}^{10}_{5}B + {}^{1}_{0}n \rightarrow \begin{cases} 6\%:\ {}^{7}_{3}Li(1.015\ MeV) + \alpha(1.777\ MeV) \\ 94\%:\ {}^{7}_{3}Li\ (840\ keV) + \alpha(1.470\ MeV) \end{cases}$$

$$b)\ {}^{6}_{3}Li + {}^{1}_{0}n \rightarrow {}^{4}_{2}He(2.05\ MeV) + {}^{3}_{1}H(2.73\ MeV)$$

$$c)\ {}^{157}_{64}Gd + {}^{1}_{0}n \rightarrow {}^{158}_{64}Gd + \gamma + conversion\ electron(\sim 70\ keV) + 7.9\ MeV$$

Equation 1. Transmutation reactions of the three most relevant elemental isotopes used for thermal neutron capture and their respective generated products. a) ^{10}B, b) ^{6}Li and c) ^{157}Gd thermal neutron capture equations.

Planar Si-detectors have nominal thermal neutron detection efficiencies of ~4%.[10,12,16] To increase this efficiency trenches etched into the silicon at various aspect ratios and backfilled with enriched ^{10}B powder can be implemented. This results in a larger active surface area and increased thermal neutron detection efficiencies.[10,14,16] The increased efficiency is the result of the larger surface area that allows higher neutron capture probability in the volume enhanced by the ^{10}B-filled trenches.[14] The higher natural thermal neutron capture cross section of ^{10}B and compatibility with Si-based technology make this material ideal for neutron conversion material. Additionally, the boron isotope can be used for conformal doping of the sidewalls to enable surface state passivation in the walls of the trenches that results in a continuous diode structure over the entire geometry of the sensor. The low surface states allow higher charge collection efficiency and reduces reverse leakage current that results in improved sensor efficiency.[10,14,16,17] Conformal doping of the sidewalls also allows a uniform electric field within the Si trench wall.[16,17]

In this paper we demonstrate a microstructured thermal neutron detector (MSND) enabled by novel and high fabrication yield boron backfilling techniques and diode fabrication methods. The integrated sensor shows consistent and reproducible efficiencies higher than 20% and, more importantly, the fabrication method enables scaling of large active areas. Our group previously reported a backfilling centrifugation technique with intrinsic efficiencies of about 20% for Si trench depths of 40 um. However, the reported process is time consuming and expensive since it requires complex centrifugation systems.[16] Furthermore, only a certain number of devices can be centrifuged at one time. The sedimentation process demonstrated here allows for flexible, reproducible, and scalable fabrication of thermal neutron sensors that is reproducible for microstructured diodes as large as 210 mm^2 with no practical limit on the number of diodes than can be filled in each batch. This process was demonstrated in with 4-inch Si-wafers with 21 sensors with an average post fabrication yield >90%. The yield was defined as sensors with efficiencies > 20%.

Furthermore, the diode fabrication methods enable contact deposition that occurs prior to backfilling to eliminate potential contamination to the Si diode surface after backfilling. This is particularly important because diode processing require diffusion anneals at temperatures > 900°C. The new method also includes Titanium Nitride (TiN) as contact that maximized the stability of the fabrication when Si-related etchants, such as piranha and hydrofluoric acid, are used in the fabrication process. The demonstrated sensors are, in this way, compatible with standard Si-manufacturing methods.

1. Results and Discussion:

Monte-Carlo Nuclear Particle (MCNP) simulations were initially performed to evaluate the expected thermal neutron detection efficiencies as function of silicon fin and trench dimensions as well as boron filling densities. A unit cell was created in MCNP with the geometry shown in Figure 1, with a target depth of a 40 µm, a Si fin of 3 µm, with the trench openings or the spacing between each Si fin was then evaluated. This unit cell was then reproduced with the actual physical dimensions of the diodes. For the simulation, an isotropic thermal neutron source was positioned at an angle normal to the surface of the detector. Figure 1 clearly shows that the optimum trench distance should be ~ 3 µm. Longer trench wall distances results in lower alpha particles reaching the silicon fin because the mean path length of the alpha particles resulting from the interaction with ^{10}B is about 3.6 µm.[16,18] Not surprisingly, the thermal neutron efficiency increases with boron filling density. None of the backfilling methods can result in a 100% filling. This is due to the fact that the powder itself has a distribution of particle sizes (with an average of < 1 micron) and irregular shapes that do not conform perfectly to the volume of the etched trench. The simulations predicts that for a 100% filled trench with opening of 2-3 µm, the expected thermal neutron detection efficiency is about 31%.

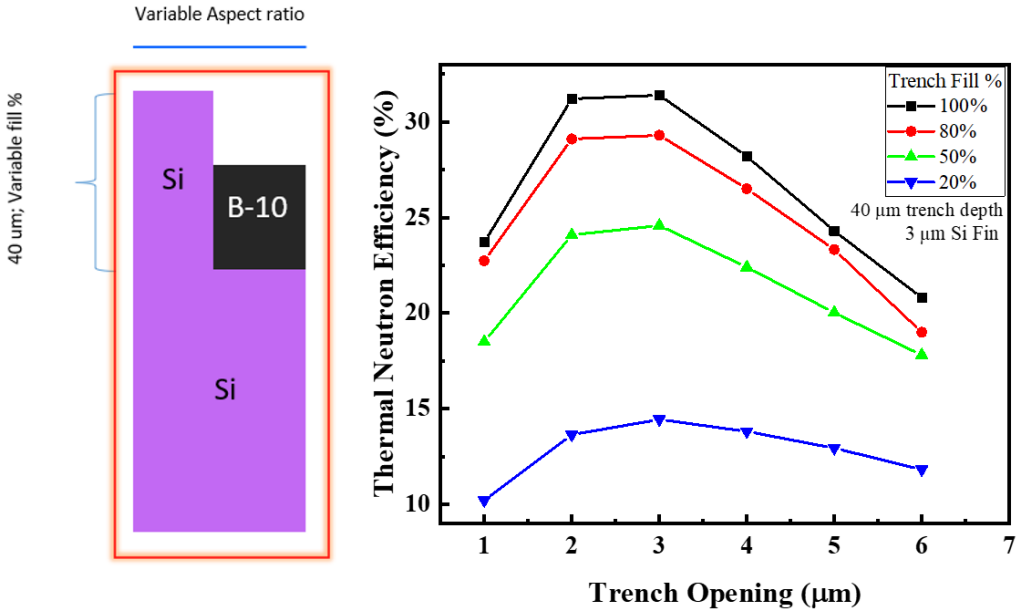

Figure 1. (left) Cross-section of the MCNP Unit cell used to simulate the diodes fabricated. (right) Thermal Neutron Detection Efficiencies (TNDE) as a function of the filling depth and trench opening

Figure 2 shows SEM images of the trenches after etching but before filling. A 3 µm trench opening and 3 µm Si-fin was selected from the simulation results shown in Figure 1. The trenches are well defined and uniform with depths of ~ 40 µm. It is to be noted that some bottling effects occur. In Figure *2*b shows the discrepancy of about 0.5 µm in wall thickness at the top of the Si trench was compared to the base of the trench. This effect is expected as the top surface is more exposed to the iterative plasma etching process to achieve targeted depths. Deeper trenches are possible but the cost in processing time and the gain related to detection efficiency are minimal. The targeted dimensions were achieved and uniform over the entire surface of a 4-inch wafer. Figure 2c shows the fully processed 4-inch wafer.

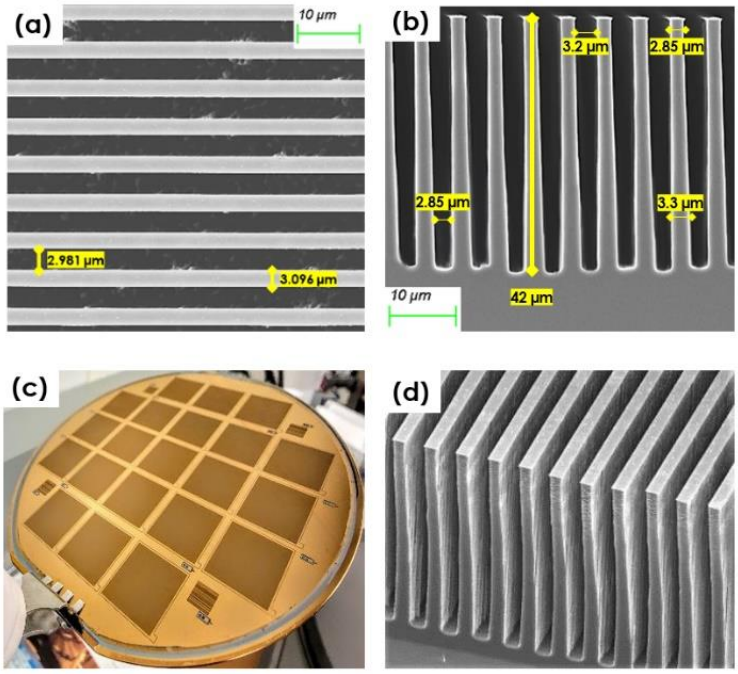

Figure 2. a) Top view SEM image of Si surface of microstructured neutron detectors. b) Cross-Section SEM view showing the dimensions of the trenches, both the targeted aspect ratio of 3 x 3 µm and a trench depth of ~ 40 µm. c) Full wafer of 21 completed detectors within the 4-in Si wafer, and (d) Off-angle SEM showing aspect ratio and uniformity of the plasma etched Si within the detector surface

Gravity assisted sedimentation is a very simple backfilling technique that consists of submerging the individual microstructure diode in a ^{10}B. This process is carried out in a solvent hood to allow the solvents to controllably evaporate resulting in a uniform boron sediment in the trenches. The static nature of this technique as well as the particle size distribution might compromise filling uniformity. To improve uniformity, the filling process was also performed under controlled agitation using an orbital shaker. In the orbital shaker method, the devices are filled using the sedimentation method described above but the devices and solution are placed on an orbital shaker at 60 RPM for 48 hours at room temperature. To further reduce the time and amount of solution used in the process, an aerosol backfilling method was also implemented. The aerosol assisted methods use the same backfilling solution but in reduced volume. The aerosol-based filling is performed using a manual spray coater at room temperature at a pressure of 20 psi using N_2 gas. Continuous layers of the ^{10}B solution are sprayed onto single devices normal to the surface.

Figure 3 compares the filling density and uniformity of the three methods described. Clearly, gravity assisted sedimentation is the least effective in filling depth and density when compared to the other methods. The orbital shaker method has a stark advantage in regard to the filling uniformity and density. While the aerosol backfilling also resulted in a full fill of the trench depths, when compared to the orbital shaker, the filling uniformity is lacking as it possesses a higher degree of trench voids or gaps in the fill. Additionally, the aerosol method adds a layer of boron on top of the detector with a thickness around 4 – 5 µm. While this can be beneficial in terms of adding a subsequent neutron converting layer to reside on top of the Si trenches, it is difficult to control the resulting thickness. If the thickness of this extra layer is too large, it may have detrimental effects to the overall neutron detection efficiency due to the alpha particle's mean path length within ^{10}B is about 3.6 µm.[16,18] Coupled with the voids in the fill will show its effect when we discuss the thermal neutron efficiencies and compare them to the orbital shaker method.

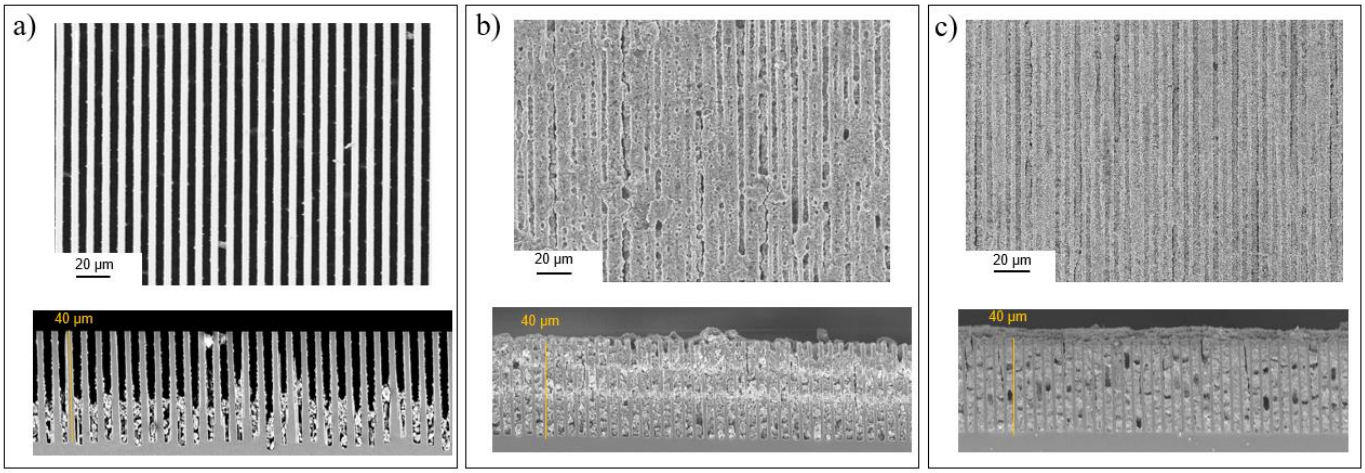

Figure 3. a) Gravity assisted sedimentation: Top-view and cross-section SEM results showing incomplete filling. b) Orbital Shaker sedimentation Top-view and cross section depicting filling showing improved filling and uniformity with minimal voids present within the Si trenches and c) Aerosol backfilling method showing uniform filling but still possessing larger number of voids and with an additional ^{10}B layer residing on the surface of the detector.

The completed diodes were characterized before and after dicing using the reverse leakage current as the figure of merit. The reverse leakage was selected because this is the parameter that most influences the lower-level discriminator or LLD of the signal. We have identified leakage currents > 8 x 10^{-5} A as the upper limit. Higher leakage current will result in higher LLD to reduce the dead time of the detector. The dead time refers to the minimum time interval required to separate two consecutive counts as individual events. The preferred LLD setting selected produces a dead time of less than 10% of the 1-hour exposure time during the irradiation experiments. A dead time of 0% is preferred but unrealistic.

Microstructured detectors normally have higher electrical noise compared to planar diodes. Noise impacts the background signal when a source is not present and higher reverse bias leakage will result in higher levels of background noise at higher channel numbers. This will compromise low energy signals that may be produced during the irradiation and impact the overall detection efficiency. Higher leakage current can be a consequence of the aggressive etching process used to fabricate silicon trenches. This produces defects into the trenches that create surface states that results in high charge recombination degrading charge collection efficiency.[14,16]

Figure 4 shows the influence of the post ^{10}B backfilling anneal – utilizing the orbital shaker method – in the I-V characteristics of the didoes. Conformal doping of the sidewalls facilitated by the high temperature anneal (950°C) of the discrete diodes enables a reduced leakage current of 10x. The red and grey lines correspond to the before and after post filling anneal, respectively. For reference, a planar device – a non microstructured diode is also shown (dashed blue line). After the high temperature anneal microstructured diodes have similar leakage current as a planar diode. This supports the hypothesis that continuous conformal doping enabled by the high temperature anneal reduces surface states originated during the Si trench fabrication. The C-V results do not show a drastic change which is positive to eliminate any parasitic capacitance that may compromise diode performance. There is an apparent reduction of capacitance at a reverse bias of -5V. This is attributed to the conformal sidewall doping that passivate surface states generated by the aggressive vertical etching.[16,17,19] Still, the small overall increase in capacitance suggests that the anneal does not heal 100% of the defects created during the etch process.

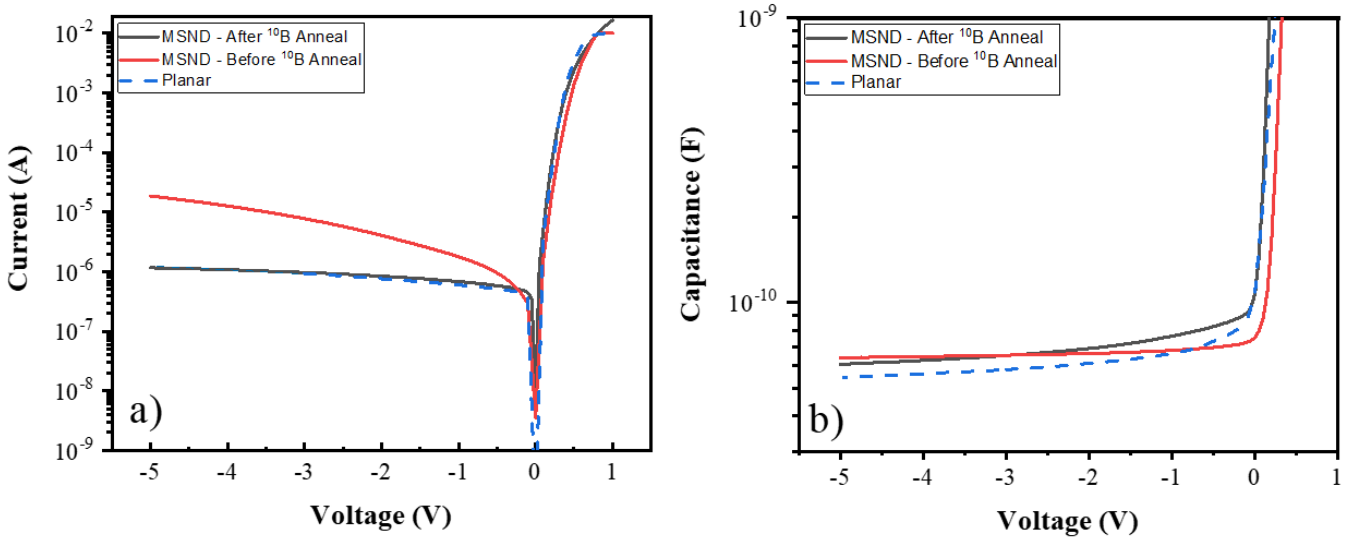

Figure 4. a) I-V curves of the microstructured neutron detectors (MSND) post fabrication, but prior to ^{10}B conformal doping anneal (red). After conformal doping anneal (black). (b) C-V curves of the microstructured diodes post fabrication but prior to ^{10}B conformal doping anneal (red), after conformal doping anneal (black). Planar style devices incorporated into each plot for reference (Dashed-blue).

Figure 5 compares the thermal neutron detection spectra for the three backfilling methods. As demonstrated by the MCNP simulations the filling density and uniformity of the ^{10}B powder in the trenches directly impact the thermal neutron detection efficiency, as observed in the experimental results for devices exposed to a Cf-252 moderated neutron source for 1 hour.

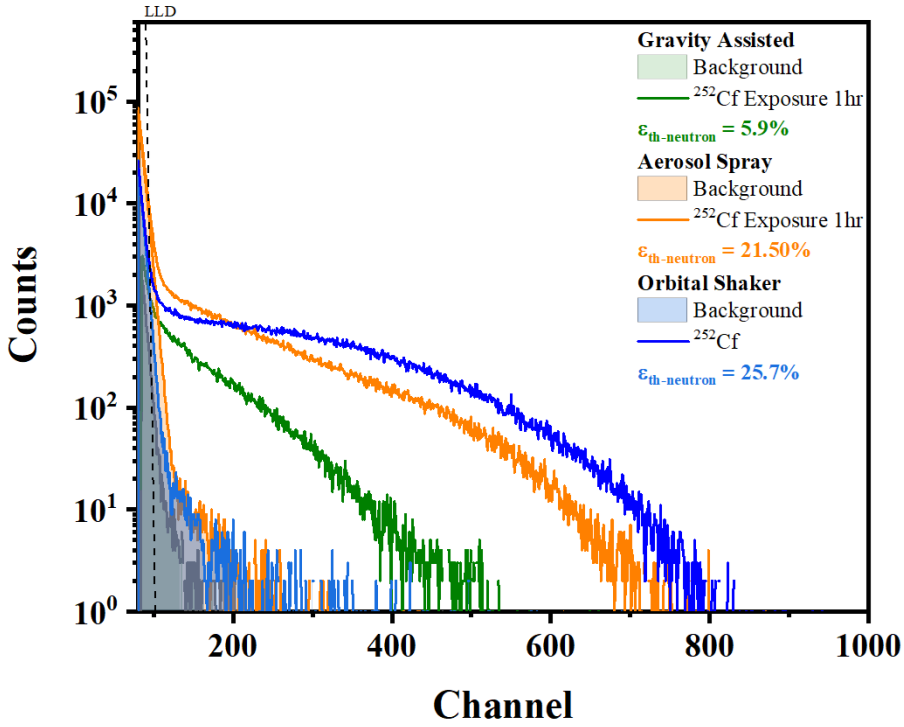

Figure 5. Thermal Neutron efficiencies of Gravity assisted sedimentation microstructured diodes (Olive), Backfilled by aerosol spray (Orange), and backfilled by Orbital Shaker (Blue). Each device's background spectra and exposure spectra consisting of 1 hour each.

The gravity assisted sedimentation method results in a thermal neutron efficiency of only 6%. While higher than the detection efficiency of a planar diode, the detection efficiency improvement is marginal. Regardless, this shows that the trenches, even in the event of poor filling yields better efficiency than planar devices. The orbital shaker and aerosol boron filling methods result in thermal neutron detection efficiencies > of 20%. The lower efficiency for the aerosol methods compared to the orbital shaker is related to a lower density of the boron in the trenches. Nevertheless, the aerosol process is highly reproducible and substantially reduces the trench filling time from 72 hours to 3-4 hours; a reduction of about 20x. The simulated vs. experimental efficiencies for low filling are varied. This outcome can be explained by the fact that the simulation assumes perfectly uniform and dense (void free) filling of the three-dimensional trench geometry. This however is an idealization that when compared to the SEM images in Figure 3, it can be seen again that various voids appear in the fill detracting from optimal efficiency gains. This is because the ^{10}B powder itself has a distribution of particle sizes in various irregular shapes affecting the density of the fill.

The results of the orbital shaker sedimentation outperformed the other two filling techniques with a detection efficiency of 25%. For a depth of only 40 μm, this possesses one of the higher detection efficiencies to etch-depth ratios of 0.625. This can be compared to McGregor D.S. et al and Wu Jia-Woei et al that contain etch depths of hundreds of microns deep with ratios of only 0.29 (backfilled with ^{6}LiF) and 0.26 (backfilled with ^{10}B) respectively.[10, 17]

2. Experimental:

2.1 Si Microstructured P-I-N Homojunction Diode Fabrication process:

A single-side polished intrinsic float-zone Si (100) wafer with resistivity > 10,000 Ohm-cm is used as the substrate. 500 nm of is thermally grown silicon-oxide (SiO_2) to act as a diffusion blocking layer for backside N-type diffusion doping. The wafer then undergoes an RCA clean to remove any excess contaminants on the surface prior to the backside N-type doping. The wafer is then immediately transferred to a solid-source diffusion ion implantation doping process that includes annealing at 950°C for 30 minutes. The next step is the interlayer dielectric (ILD) deposition. The ILD has two purposes: 1) to again prohibit the diffusion of the subsequent front side doping, and 2) to provide protection to the top surface of the wafer while being patterned for device active areas by photolithography. The ILD is defined by 200 nm thermally grown SiO_2 followed by 50 nm Silicon Nitride deposition using low-pressure chemical vapor deposition (LPCVD).

A conventional photolithography process is utilized to define the P-type regions of the diode. The front side is then patterned using S1813 photoresist and the ILD and oxide is etched to expose the regions to be P-type doped. An additional RCA cleaning procedure is performed to again eliminate any potential contaminants that could later be diffused in the open vias. Immediately afterwards, Borofilm-100 spin on glass (SOG) is deposited on the front side of the wafer. The wafer is then soft baked at 200°C for 20 minutes to remove any excess solvents. After the soft bake, the wafer is transferred to a tube furnace at 950°C for 30 minutes in ultra-high-purity (UHP) N2 ambient to diffuse boron into the top silicon layer. The remaining SOG on the surface of the wafer is removed using BOE until the regions become hydrophobic.

200 nm of TiN is deposited on the front side of the wafer by reactive sputtering of a Titanium target in an ambient of 5% Nitrogen/Argon at a chamber pressure of 2 mTorr. The deposition power used was 250 W in an RF gun with a sputtering rate of 3.5 nm/min. Subsequently, the hard mask is deposited (100 nm of AlSi) in-situ with the top contact deposition. The hard mask serves as a protective layer of the fins or regions of silicon that are not to be removed. The targeted trench dimensions both Si fin and trench opening are defined by traditional photolithography processes. After trench patterning, a deep silicon etch (DSE) with SF_6 and C_4F_8 gases at a temperature of 180°C is used for the silicon. This etching process is known as the Bosch process where the alternating gases provide the gaseous etchant and passivation pulses to allow uniform columnar Si etching.[19] Figure 6 shows a schematic of the fabrication process within the diode area and how the Si trenches are generated from the metallized contact and AlSi hard mask. It is paramount that the pulses of the etching gases are optimized with correct timings and flow. Ignorance of this step may cause irregular etching depths, unintended targeted dimensions of trench widths, and or non-uniform trench geometries throughout the depth i.e. narrow features near the bottom of the trench and wider openings on top.

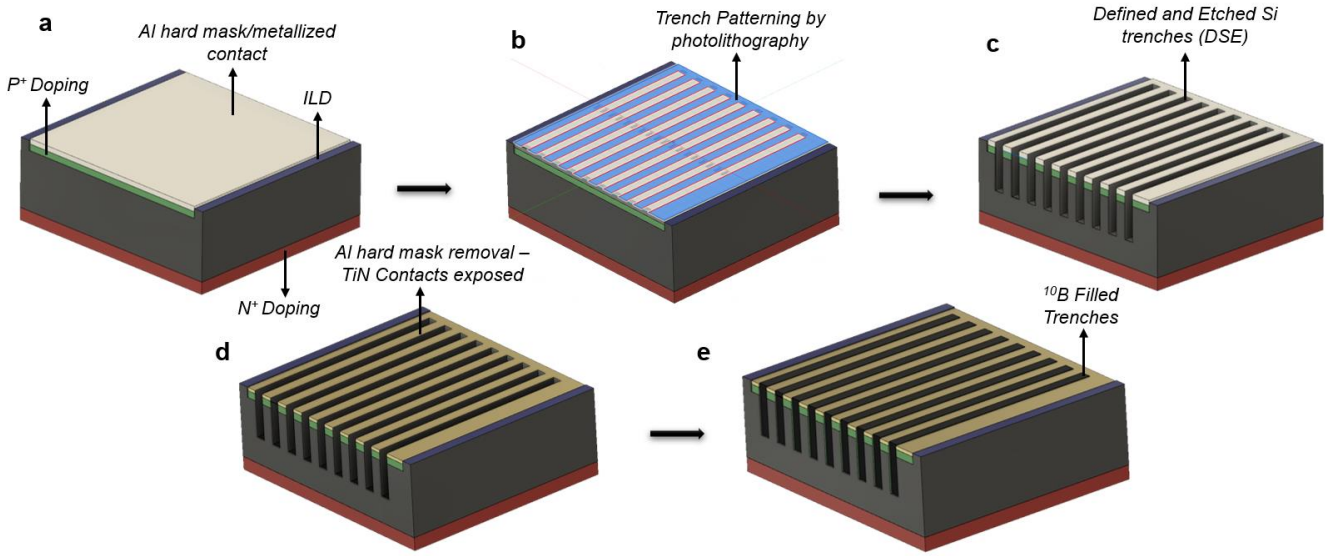

Figure 6. (a) Si diode planarized with Al hard mask and contact. (b) Defined trench microstructure by photolithography (blue) on Al hard mask layer and develop. (c) Plasma etched trenches into Si through Al hard mask. (d) Wet etching of Al hard mask to reveal TiN contact layer underneath. (e) Boron filled microstructured trenches

The backside of the wafer is then prepped for metallization by removing the ILD nitride layer by reactive ion etching (RIE) followed by the oxide removal in BOE until the surface is hydrophobic. The same 250 nm TiN contact deposition is repeated for the rear of the wafer by RF reactive sputtering. Once complete, the devices are ready to be tested as-is within the wafer; that is, without any boron backfilling. Once the devices are diced individually, they are ready to be backfilled and conformally doped in a high temperature anneal which will be mentioned in the next sub-section.

2.2 Trench Backfilling Process:

The backfilling process uses a solution of enriched ^{10}B powder with average particle size (APS) less than 1 μm, acetone, ethanol, isopropanol alcohol, and the polymer polyvinylpyrrolidone (PVP) which is used as a surfactant. [20,21] The smaller the particle size the better the filling should be as the small particles should easily fit in narrowly etched silicon trenches. Three backfilling methods are reported in this paper: Traditional gravity-assisted sedimentation, sedimentation by cyclic movement of an orbital shaker, and lastly aerosol assisted backfilling using a pressurized spray coater. All three are discussed and compared for their filling uniformity and their impacts on thermal neutron detection.

To fill the trenches, a solution of enriched ^{10}B powders, acetone, ethanol, and isopropanol alcohol were prepared, as shown in Table 1.

Table 1: Enriched ^{10}B Solution Components

Acetone	IPA	Ethanol	Enriched Boron
4.8 mL	7.1 mL	9 mL	28 mg

The enriched ^{10}B powder was obtained from 3M with a purity of 96% and average particle size (APS) of < 5 microns. To further reduce the particle size, an additional ball milling step is required to reduce the APS to < 1 micron. This is important as small particles will enable uniform filling and minimizes blocking out the trenches by large, agglomerated particles. The solution is next rod sonicated for 30 minutes to achieve a homogenous powder dispersion.

Once the devices are backfilled, the next step is the boron diffusion into the sidewall trenches. For this process, the contact areas on the perimeter of the devices are carefully cleaned from any residual boron powder using IPA. The devices are then annealed at 950°C in Ar atmosphere for 15 minutes. This high temperature post fabrication annealing enables a conformal doping process of the boron powders inside the trench walls.[16,17] This sedimentation not only fills the structures well but also allows for a thin 2 μm layer on top of the devices. This is sufficient to act as a top neutron conversion layer while being thin enough for the generated alpha particle reach the Si.[22]

2.3 Neutron Sensing Evaluation:

A moderated Cf-252 neutron source was used and housed in water extended polyester shielding (WEPS). Thermal neutron flux is ~ 762,000 n/(hr-cm^2) at the device location. An Ortec 142A preamplifier is used for preamplification and negative bias voltage of -5V to ensure the diode is in reverse biased conditions possessing a large depletion region for alpha particle capture. Once a thermal neutron strikes the ^{10}B, a 1.4 MeV alpha particle emits into the silicon and a pulse is generated which can be seen in an oscilloscope. Pulse shaping was performed in an Ortec 575 shaping amplifier. The signal is passed to an Ortec EASY-MCA-2K multi-channel analyzer was used to generate the channel/energy spectra via PC. Efficiency calibrations were based on a commercially bought neutron detector – Domino™ Neutron detector from RDT – with a known

thermal neutron efficiency of 30% per manufacturer specification sheets. Our fabricated and tested devices are then normalized to this performance for thermal neutron efficiency calculations.

3. Conclusions:

We have shown the fabrication techniques of the Si wafer processing for high efficiency Si microstructured thermal neutron detectors (MSNDs). The wafers possess high yield in the fabrication process of etching 40 μm deep trenches with leakage current densities within our tolerance for neutron detection of 4.76 x 10^{-9} A/mm^2. Three enriched ^{10}B solution based backfilling processes have been discussed by means of gravity assisted sedimentation, orbital shaker sedimentation, and aerosol coating that show a range in uniformity in the devices they have filled with trench depths of 40 μm. Thermal neutron detection efficiencies (TNDEs) have achieved upwards of 25% compared to the simulated theoretical efficiency of 31% for the same detector dimensions, aspect ratios, and trench depth. Discrepancy in the efficiency values can be attributed to idealization in the simulation which assumes a perfect solid filling of the structures. In reality, the filling techniques leave ^{10}B particles in a randomly distributed fill containing irregular shapes thus detracting from a perfect fill. Backfilling the detector using cyclical agitation sedimentation by use of an orbital shaker retained most of its theoretical efficiency which resulted in the most uniform fill across the detector possessing the least number of voids when compared to the aerosol method. When compared to non-agitated gravitational assisted sedimentation, this method performed with the least amount of filling and uniformity. Because of which, this resulted in the least amount of thermal neutron detection comparable to a planar Si detector (~6%).

The conformal doping process by post fabrication high temperature annealing shows an enhancement in the reverse bias leakage current. This improvement is seen in the reduction of the reverse bias leakage current from 2 x 10^{-5} A – 1 x 10^{-6} A, providing similar levels of reverse leakage current to that of the planar diode and allowing for lower levels of noise in the detector than can be attributed to excess gamma irradiation from the Cf-252 source. The devices also possess four orders of rectification with a forward bias on-state current of 1 x 10^{-2} A. With this reduction in leakage current to levels near of a pristine substrate (planar) detector coupled with the success in enriched ^{10}B sedimentation backfilling, these detectors possess one of the higher thermal neutron detection efficiency to trench depth ratios of 0.625. With this filling success, target depths are only limited to filling time and scaling of enriched ^{10}B solution. Both of which can be utilized for full wafer thermal neutron detection fabrication with a path towards commercialization.

Author Contributions

The manuscript was written by Zeshaan Shamsi with contributions from all authors. All authors have given approval to the final version of the manuscript.

Funding Sources

Department of Homeland Security (DHS)

ACKNOWLEDGMENTS

The authors would like to thank the Department of Homeland Security (DHS) for their support, oversight, and participation in this project's success.

REFERENCES

(1) Kouzes, R. T.; Ely, J. H.; Erikson, L. E.; Kernan, W. J.; Lintereur, A. T.; Siciliano, E. R.; Stephens, D. L.; Stromswold, D. C.; Van Ginhoven, R. M.; Woodring, M. L. Neutron Detection Alternatives to 3He for National Security Applications. Nucl. Instrum. Methods Phys. Res. Sect. Accel. Spectrometers Detect. Assoc. Equip. 2010, 623 (3), 1035–1045. https://doi.org/10.1016/j.nima.2010.08.021.

(2) Muminov, R. A.; Tsvang, L. D. High-Efficiency Semiconductor Theramal-Neutron Detectors. Sov. At. Energy 1987, 62 (4), 316–319. https://doi.org/10.1007/BF01123372.

(3) Davidson, T. A.; Emerson, D. E. Method and Apparatus for Direct Determination of Helium-3 in Natural Gas and Helium; U.S. Department of Interior, Bureau of Mines, 1990.

(4) Ahmed, S. N. Physics and Engineering of Radiation Detection; Academic Press, 2007.

(5) Dunning, J. R.; Pegram, G. B.; Fink, G. A.; Mitchell, D. P. Interaction of Neutrons with Matter. Phys. Rev. 1935, 48 (3), 265–280. https://doi.org/10.1103/PhysRev.48.265.

(6) NaI TI scintillation crystal, Thallium doped Sodium Iodide scintillation crystal, NaI TI scintillator diameter 1 inch x 1 inch. http://www.epic-scintillator.com/NaI-scintillator-1inchx1inch (accessed 2022-10-18).

(7) NaIL Scintillation Crystals | Crystals. https://www.crystals.saint-gobain.com/radiation-detection-scintillators/crystal-scintillators/nail-scintillation-crystals (accessed 2022-10-18).

(8) Yang, P.; Harmon, C. D.; Doty, F. P.; Ohlhausen, J. A. Effect of Humidity on Scintillation Performance in Na and Tl Activated CsI Crystals. IEEE Trans. Nucl. Sci. 2014, 61 (2), 1024–1031. https://doi.org/10.1109/TNS.2014.2300471.

(9) Ahmed, S. N. 5 - Solid-State Detectors. In Physics and Engineering of Radiation Detection (Second Edition); Ahmed, S. N., Ed.; Elsevier, 2015; pp 259–329. https://doi.org/10.1016/B978-0-12-801363-2.00005-X.

(10) McGregor, D. S.; Bellinger, S. L.; McNeil, W. J.; Unruh, T. C. Micro-Structured High-Efficiency Semiconductor Neutron Detectors. In 2008 IEEE Nuclear Science Symposium Conference Record; IEEE: Dresden, Germany, 2008; pp 446–448. https://doi.org/10.1109/NSSMIC.2008.4775204.

(11) Shultis, J. K.; McGregor, D. S. Efficiencies of Coated and Perforated Semiconductor Neutron Detectors. IEEE Trans. Nucl. Sci. 2006, 53 (3), 1659–1665. https://doi.org/10.1109/TNS.2006.872639.

(12) Bellinger, S. L.; Fronk, R. G.; McNeil, W. J.; Sobering, T. J.; McGregor, D. S. Enhanced Variant Designs and Characteristics of the Microstructured Solid-State Neutron Detector. Nucl. Instrum. Methods Phys. Res. Sect. Accel. Spectrometers Detect. Assoc. Equip. 2011, 652 (1), 387–391. https://doi.org/10.1016/j.nima.2010.08.049.

(13) Fronk, R. G.; Bellinger, S. L.; Henson, L. C.; Huddleston, D. E.; Ochs, T. R.; Sobering, T. J.; McGregor, D. S. High-Efficiency Microstructured Semiconductor Neutron Detectors for Direct 3He Replacement. Nucl. Instrum. Methods Phys. Res. Sect. Accel. Spectrometers Detect. Assoc. Equip. 2015, 779, 25–32. https://doi.org/10.1016/j.nima.2015.01.041.

(14) McGregor, D. S.; Bellinger, S. L.; Shultis, J. K. Present Status of Microstructured Semiconductor Neutron Detectors. J. Cryst. Growth 2013, 379, 99–110. https://doi.org/10.1016/j.jcrysgro.2012.10.061.

(15) Mireshghi, A.; Cho, G.; Drewery, J. S.; Hong, W. S.; Jing, T.; Lee, H.; Kaplan, S. N.; Perez-Mendez, V. High Efficiency Neutron Sensitive Amorphous Silicon Pixel Detectors. IEEE Trans. Nucl. Sci. 1994, 41 (4), 915–921. https://doi.org/10.1109/23.322831.

(16) Nandagopala Krishnan, S. S.; Avila-Avendano, C.; Shamsi, Z.; Caraveo-Frescas, J. A.; Quevedo-Lopez, M. A. 10 B Conformal Doping for Highly Efficient Thermal Neutron Detectors. ACS Sens. 2020, 5 (9), 2852–2857. https://doi.org/10.1021/acssensors.0c01013.

(17) Wu, J.-W.; Weltz, A.; Koirala, M.; Lu, J. J.-Q.; Dahal, R.; Danon, Y.; Bhat, I. B. Boron-10 Nanoparticles Filled Silicon Trenches for Thermal Neutron Detection Application. Appl. Phys. Lett. 2017, 110 (19), 192105. https://doi.org/10.1063/1.4983289.

(18) Shao, Q.; Voss, L. F.; Conway, A. M.; Nikolic, R. J.; Dar, M. A.; Cheung, C. L. High Aspect Ratio Composite Structures with 48.5% Thermal Neutron Detection Efficiency. Appl. Phys. Lett. 2013, 102 (6), 063505. https://doi.org/10.1063/1.4792703.

(19) Laermer, F.; Schilp, A. Method of Anisotropically Etching Silicon. 5501893, March 26, 1996. https://www.freepatentsonline.com/5501893.html#google_vignette (accessed 2022-10-18).

(20) Baccaro, S.; Pajewski, L. A.; Scoccia, G.; Volpe, R.; Rosiak, J. M. Mechanical Properties of Polyvinylpyrrolidone (PVP) Hydrogels Undergoing Radiation. Nucl. Instrum. Methods Phys. Res. Sect. B Beam Interact. Mater. At. 1995, 105 (1–4), 100–102. https://doi.org/10.1016/0168-583X(95)00519-6.

(21) Königer, T.; Münstedt, H. Influence of Polyvinylpyrrolidone on Properties of Flexible Electrically Conducting Indium Tin Oxide Nanoparticle Coatings. J. Mater. Sci. 2009, 44 (11), 2736–2742. https://doi.org/10.1007/s10853-009-3357-3.

(22) McGregor, D. S.; Klann, R. T.; Gersch, H. K.; Yang, Y. H. Thin-Film-Coated Bulk GaAs Detectors for Thermal and Fast Neutron Measurements. Nucl. Instrum. Methods Phys. Res. Sect. Accel. Spectrometers Detect. Assoc. Equip. 2001, 466 (1), 126–141. https://doi.org/10.1016/S0168-9002(01)00835-X.